


 Cite this: *RSC Adv.*, 2025, 15, 714

Research progress on and outlook of direct CO₂ thickeners for enhanced oil recovery

 Yuxuan Song,^{ID ab} Qun Zhang,^{*ab} Xinyuan Zou,^b Jian Fan,^b Sicai Wang^{ab} and Yan Zhu^{ab}

Supercritical CO₂, as an environmentally friendly and pollution-free fluid, has been applied in various EOR techniques such as CO₂ flooding. However, the low viscosity of the gas leads to issues such as early breakthrough, viscous fingering, and gravity override in practical applications. Although effective mobility-control methods, such as CO₂ WAG (water alternating gas)-, CO₂ foam-, and gel-based methods, have been developed to mitigate these phenomena, they do not fundamentally solve the problem of the high gas-oil mobility ratio, which leads to reduced gas sweep efficiency. Adding CO₂ direct thickeners to displacing fluid can increase its viscosity, achieve deeper mobility control, and thus improve the CO₂ flooding oil-recovery effect. Unlike other methods, direct thickeners can alter the physical and chemical properties of CO₂, making it a fundamentally effective means of achieving mobility control. This approach can be applied in various reservoir environments and formations, or it can assist other methods for more in-depth mobility control. This article reviews the development and application of CO₂ direct thickeners and introduces the thickening mechanisms and effects of different types of thickeners as well as their existing problems and future development directions.

 Received 11th October 2024
 Accepted 14th November 2024

DOI: 10.1039/d4ra07300b

rsc.li/rsc-advances

1. Introduction

With the development of the global economy, the world's oil consumption has increased significantly, but the production of crude oil is decreasing. The optimization and development of oil extraction technology are therefore urgent priorities.¹ Typically, primary and secondary oil recovery can only recover about 40% of a reservoir's reserves; thus, the development of tertiary oil-recovery technology is crucial for maintaining crude oil production and reducing oil imports. CO₂ flooding is one of the most promising technologies in enhanced oil recovery (EOR), characterized by its non-toxic and environmentally friendly nature, abundant availability, chemical stability, and ease of miscibility with crude oil. Additionally, CO₂ can be stored in subsurface pores, achieving integrated oil displacement and storage during the oil displacement process.²⁻⁴ Since the 1960s, the United States has successively carried out a series of studies on CO₂ flooding, and there have been more than 130 commercial CO₂ flooding projects to date.⁵ According to statistics, the annual production of CO₂ flooding in the U.S. reached 137.1 million tons in 2014, accounting for about 93% of the world's total CO₂ flooding production.⁶ Recently, China proposed the "dual-carbon" goal, where carbon dioxide capture, utilization, and storage (CCUS) is a primary method for end

offsetting. CO₂ flooding holds significant application value as a vital component of CCUS.⁷⁻⁹

Gases have better diffusive capabilities in porous media and tend to enter larger pores first, offering significant permeability at lower gas saturations. However, the high mobility ratio between CO₂ and crude oil results in an unstable displacement front, causing early breakthrough, and this problem is exacerbated by increased heterogeneity within the reservoir.¹⁰ Moreover, problems such as gravity override and hindered oil-gas mixing and reactivity can significantly reduce sweep efficiency and oil displacement efficiency.^{11,12} Therefore, reducing the two-phase mobility ratio and strengthening the mobility control of CO₂ are critical issues that need to be addressed to improve the oil-recovery rate of CO₂ flooding technology.

CO₂ thickening is an effective way to reduce the mobility ratio between the oil and gas phases. Due to the low critical temperature (31.1 °C) and critical pressure (7.38 MPa) of CO₂, most reservoir temperatures and pressures exceed the critical conditions for CO₂, and it often exists in a supercritical state within the reservoir.¹³ Supercritical carbon dioxide (scCO₂) possesses superior heat transfer and diffusive properties, and its density is akin to liquid-state substances, which contribute to its enhanced solvent performance. Dissolving polymers in scCO₂ and utilizing the non-bonding forces between solute molecules to form a large molecular network can significantly increase the viscosity of CO₂.¹⁴

CO₂ direct thickeners are not only applicable for EOR processes but also can be widely used in scCO₂ fracturing fluids

^aInstitute of Porous Flow and Fluid Mechanics, Chinese Academy of Sciences, Langfang, Hebei, 065007, China

^bResearch Institute of Petroleum Exploration and Development, Beijing, 100083, China



to enhance the sand-carrying capacity of the fracturing fluid, as well as in other related fields, such as CO₂ adsorption. Therefore, the development of a high-performance CO₂ direct thickener is vital for the entire EOR field. This paper presents a review of CO₂ direct thickeners from a molecular perspective, as well as their dissolution thickening mechanisms and application conditions. An outlook on the development prospects of CO₂ direct thickeners is also provided as well as insights offering technical support for their future practical application in oil fields.

2. CO₂ thickening

2.1 CO₂ mobility control and CO₂ thickening

It is essential to control the mobility of the gas in the reservoir to alleviate problems such as gas loss and poor sweep efficiency caused by gas channeling. CO₂ mobility control can be achieved through three main approaches: First, by reducing the gas saturation and permeability to stabilize the displacement front and alter the flow pattern in the formation. Second, by altering the formation permeability to enhance the control over the flow path of CO₂ within the reservoir. Third, by increasing the gas viscosity to reduce the mobility ratio between the oil and gas phases.^{10,15,16} Based on these principles, CO₂-mobility-control methods mainly include water-alternating-gas (WAG), CO₂ thickening, CO₂ foam, and gel methods, with each method offering certain advantages and disadvantages, as shown in Table 1.^{17–19}

2.1.1 CO₂-WAG. The WAG process combines the advantages of both water injection and gas injection. The injection of water and gas can reduce the relative permeability of the gas, the interfacial tension between the displacement fluid and oil, and the capillary forces, thereby improving the mobility ratio

and adjusting the position of the gas–oil–water contact interface to increase the sweep coefficient.^{20,21} This method can enhance the recovery of the original oil or gas in place (OOIP) by an average of 5% to 10%.^{22,23}

The factors affecting the efficiency of CO₂-WAG flooding include reservoir heterogeneity, wettability, the fluid physico-chemical properties, and the injection parameters.¹⁷ The water shielding issue caused by the injection of two phases can significantly reduce the recovery rate during the WAG process, especially in formations with high water saturation levels.^{24,25} Additionally, due to the changes in relative permeability, both water and gas will experience injection losses. This issue can be alleviated by reducing the water slugs and increasing the gas slugs, but at the same time, controlling the gas mobility becomes more difficult.²⁶ The injection parameters of CO₂-WAG have a significant impact on the final recovery efficiency. Valeev and Shevelev²⁷ evaluated the effect of the water–gas injection ratio on the final recovery efficiency using a field in the Kogalym region as an example. The addition of water could reduce the mobility of CO₂, and at a certain water–gas ratio, the water–oil–gas three-phase system could attain a mixed phase in the porous medium, forming a viscous single phase, which resulted in the optimal displacement efficiency. The miscible process involved the dissolution of CO₂ into a mixture of crude oil and water and entailed very complex physicochemical reactions. However, most reservoirs cannot achieve perfect miscible conditions, and the purpose of mobility control can only be achieved through the buffering effect of water between oil and gas with high mobility ratios. To enhance the efficiency of the injection, polymers, surfactants, and nanomaterials are often incorporated to further assist the WAG process. A new technology that has emerged is the chemical enhanced water-alternating-gas (CEWAG) system, where chemical agents are

Table 1 Comparison of various CO₂-mobility-control methods

| Mobility-control method | Mechanism | Advantages | Shortcomings |
|----------------------------|--|---|--|
| CO ₂ -WAG | Alternately injecting water and gas reduces gas permeability and uses the injected water to stabilize the displacement front | High microscopic oil displacement efficiency from gas injection and high swept volume from water injection, while requiring a small amount of gas injection | Water shielding and injection losses, not suitable for oil reservoirs with high heterogeneity, injection and production parameters significantly affect EOR efficiency |
| CO ₂ foam | Forms a stable foam front at the forefront of displacement fluid, utilizing the high-viscosity characteristic of the foam to reduce the mobility of the gas, with some gas bubbles serving a plugging function | Foam has various forms of mobility-control effects | Injection is difficult, foam stability is poor, and surfactants will adsorb onto the rock surface |
| Gel | Forming a polymer gel in the formation to plug large pores and alter the formation permeability | Repairs and improves the flow channels of displacement fluid and seals off leaks | Plugging stability is poor, not shear-resistant, gel formation exhibits instability, and the effect deteriorates after multiple rounds of profile adjustment |
| CO ₂ thickening | Polymers are dissolved in supercritical CO ₂ and increase the viscosity of the gas, thereby reducing the mobility ratio | Water-free systems are easier to inject into the reservoir | High cost |



added to enhance the WAG process. These agents are primarily added to the aqueous phase, and there is less research on adding them to the gaseous phase.²¹

2.1.2 CO₂ foam. Foam has the ability to reduce the interfacial tension between two phases, increase the viscosity of the displacement fluid, stabilize the displacement front, reduce gravity segregation, and lower the relative permeability. The viscosity of foam is slightly higher than that of gas. This can not only delay the breakthrough time but also allow it to remain in some pores to perform plugging in the reservoir.²⁸ M. A. Almobarky²⁹ studied the properties and displacement efficiency of CO₂ foams generated by anionic surfactants such as AOS, and found that the surfactant adsorbed at the interface, effectively reducing the interfacial tension while stabilizing the foam, ultimately enhancing the recovery rate by 1–8.38%. During this process, the properties of CO₂ do not change; instead, it exists in the porous medium in the form of foam, achieving higher displacement efficiency. The stability of the foam is essential in CO₂ foam flooding, and there are many factors that affect its stability, such as the temperature, surfactant concentration, and system pH. Moreover, alternating injection can also impact the continuity of the foam, thereby affecting the storage efficiency of the gas.^{30–34}

Foam is a non-equilibrium system, and it will gradually collapse and disappear even without disturbance over time. The chemicals used for foaming are typically surfactants, and a continuous injection of surfactant solution is required to stabilize and continuously regenerate the foam in the reservoir.²⁹ CO₂ foam flooding has been applied in various field sites. Field experiments have shown that CO₂ foam can increase the recovery rate by at least 5%, which is significantly below the results obtained from laboratory tests showing about a 30% increase in recovery rate. The main reason is that surfactants will be extensively adsorbed in the reservoir, causing losses and preventing the continuous and stable formation of the foam.^{33,35}

2.1.3 Gel. In addition to optimizing the injection method, the injection of polymer gels to block high-permeability channels and small pores can change the formation permeability and the flow path of the displacement fluid, driving the fluid into low-permeability areas, which can also help with mobility control. The physical and chemical properties of CO₂ are not changed in this process. The underground crosslinked gel is the most widely used gel system, and the most commonly used polymer is polyacrylamide (PAM), which can undergo crosslinking reactions with various crosslinking agents, such as Cr³⁺, Al³⁺, and phenolic systems.³⁶ After crosslinking of the polyacrylamide molecules and crosslinking agents in the formation, the rheological volume of the gel increases through the hydration and electrostatic forces of the groups, enabling it to plug high-permeability channels. The formed three-dimensional (3D) reticulated structure endows the gel with a certain strength, allowing it to enter deeper into the formation. The crosslinking reaction occurs within the reservoir, and it is impossible to accurately control the gelation time, which, along with issues such as shear degradation, poses challenges. There are various types of gel systems, such as pre-crosslinked gels and foam gels. Their formation principles are essentially the

same, with differences lying in the type of gel, its strength, and the application techniques.^{37,38} Gel plugging has been extensively applied in water flooding. For instance, Brattækås³⁹ studied the leakoff and plugging effects of chromium (Cr)(III)-acetate hydrolyzed polyacrylamide gels in carbonate reservoirs and verified the position and existence of a stable displacement front. Gels have also received increasing research attention in CO₂ flooding. In one study, Wang⁴⁰ evaluated the plugging effect of a CO₂-responsive preformed particle gel (CR-PPG) in fractured sandstone cores. Experiments demonstrated that in a scCO₂ environment, CR-PPG could expand to approximately twice its original volume and it resisted a pressure of about 617 psi before breakthrough.

2.1.4 CO₂ thickening. The most direct way to reduce the migration rate of CO₂ and improve the mobility ratio is to add thickeners to CO₂, such as polyfluoropropyl acrylate, polydimethylsiloxane, or polyvinyl acetate. Thickeners can dissolve in CO₂ through the interaction between their functional groups and the CO₂ molecules, utilizing their inherently high viscosity or forming a large molecular network structure to increase the viscosity of the entire solution. This technology is different from other mobility-control methods in that it fundamentally changes the physical and chemical properties of the CO₂ system. CO₂ thickening has many advantages in the EOR process. First, the reservoir's temperature and pressure conditions can easily reach the critical point of CO₂. Second, compounds that are soluble in CO₂ are usually not soluble in water or oil, which can reduce the adsorption of polymers in the reservoir. Ideally, the thickener can increase the viscosity of scCO₂ several times or even dozens of times at an extremely low concentration of below 5 wt%. These requirements are much lower than those for the miscible conditions in WAG.

Based on different thickening mechanisms, CO₂ thickeners can be divided into direct thickeners and indirect thickeners. Direct thickeners dissolve in CO₂ to form a thermodynamically stable solution, enhancing the viscosity and density of the injected fluid. This process involves only a single phase change of CO₂ and does not require water injection, which can prevent issues like water shielding and well acidification. Indirect thickeners thicken the displacement fluid by forming CO₂ foams or emulsions with high apparent viscosity. Additionally, there is research on thickening CO₂ with nanoparticles, which involves achieving a stable dispersion of nanoparticles in CO₂. To achieve the desired viscosity, it is often necessary to modify the nanoparticles or add them together with polymers that are soluble in CO₂.

Comparing various mobility-control methods, it could be observed that CO₂-WAG, CO₂ foam, and gel all aim to control mobility by altering the flow pattern and path of CO₂ within the reservoir. These are indirect means of mobility control, as they do not change the physicochemical properties of the supercritical CO₂, nor do they fundamentally address the issue of the large viscosity gap between oil and gas. It is also challenging to achieve more precise control over the mobility of CO₂ with these methods. Direct thickeners, on the other hand, can increase the viscosity of the CO₂ system, altering the fluid's physical and chemical state, and can also assist other methods in achieving



further mobility control, making it a fundamentally effective means. Before the study of gas-soluble thickeners, water-soluble thickeners (such as polyacrylamide) had been extensively studied and applied in water flooding. CO₂ thickening technology is a challenging and breakthrough technology. The development of high-performance CO₂ thickeners represents an innovation in EOR techniques for gas flooding. Regardless of the reservoir's permeability, the saturation of the injected fluid, and the properties of the brine, a thickened CO₂ system can always play a role in mobility control.⁴¹

2.2 Dissolution and thickening mechanism

Direct CO₂ thickeners mainly include polymers, small molecule compounds, and nanoparticles.^{42–44} The principles of direct thickeners dissolving and thickening in CO₂ can mainly be divided into two types. One type is based on the interactions of small molecule compounds with functional groups on the exterior or ends of their molecular chains, which form a network structure in the solution through van der Waals forces and other electrostatic interactions that hinder the flow of CO₂ molecules and increase the viscosity of the system (Fig. 1). Most hydrocarbon thickeners and modified copolymers belong to this type. The structure formed by non-covalent interactions is very fragile and can be easily destroyed. The other type involves high-molecular-weight polymers, such as fluoropolymers and siloxane polymers, which can form a large molecular network structure and increase the viscosity by intertwining their macromolecular chains at low concentrations. However, polymers with high molecular weights are difficult to dissolve in CO₂, often requiring a significant amount of co-solvents to be added. Nanoparticles primarily increase the viscosity of solutions through surface energy effects and homogeneous dispersion.

There are three types of forces in a solution system: solute–solute interactions, solute–solvent interactions, and solvent–solvent interactions. The competition and balance among these three determine the final solubility. During dissolution, solute–solvent interactions promote the process, whereas solute–solute and solvent–solvent forces hinder it. Therefore, in polymer–CO₂ solutions, the greater the interaction force between the polymer and CO₂ molecules, the higher the solubility of the polymer in CO₂. Although the solubility of the polymer is increased, the viscosity of the solution may not necessarily be increased because the greater the affinity between the polymer and CO₂, the more inclined they are to bind, which can reduce the interactions between the polymer molecules. Similarly, if the

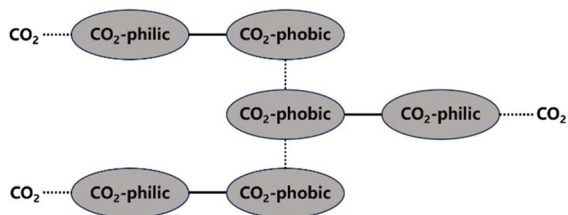


Fig. 1 Interactions between polymers and CO₂ molecules.

polymer has a high cohesive energy and strong intermolecular forces, it will preferentially interact with itself, repelling the binding with CO₂ molecules, which would result in reduced solubility. Therefore, it is necessary to ensure that there is a strong interaction between the polymer and CO₂ molecules while also maintaining a powerful interaction force between the polymer molecules (or a certain repulsive force between the polymer and CO₂) to achieve a good high-viscosity homogeneous CO₂ solution.⁴⁵

According to the requirements of intermolecular forces, direct thickener molecules need to simultaneously possess CO₂-philic groups that can increase solubility and CO₂-phobic groups that can enhance the interaction forces between polymer molecules. Atactic polymers are more soluble in CO₂ than isotactic and syndiotactic polymers.⁴⁶ Incorporating more short side chains can reduce the polymer's dissolution pressure when it contains the same number of CO₂-philic groups. This is because the increase in free volume not only enhances the mixing entropy but also improves the flexibility of the molecular chains.⁴⁷ Overall, macromolecular chains are more likely to become entangled in a solution, and the thickening ability can be enhanced with increasing the molecular volume, but it is also relatively more difficult for them to stably exist in the solution. Factors that affect the thickening effect mainly include the chemical structure, molecular weight, temperature, and pressure, as shown in Table 2.

3. CO₂ direct thickeners

3.1 Fluorinated polymers

CO₂ is a nonpolar molecule and a weak solvent for many polar substances. However, due to the presence of the C=O bond and a higher quadrupole moment within CO₂, there is an electrostatic attraction between CO₂ and polar groups, such as fluorocarbons, siloxane, and carbonyl groups. Therefore, compounds with larger polar groups can dissolve in supercritical CO₂.⁴⁸ Research has found that fluorine-containing groups have the best affinity with CO₂ and can maintain a certain solubility even at high molecular weights. Dardin⁴⁹ dissolved *n*-hexane and perfluorinated *n*-hexane in supercritical CO₂, and compared the chemical shifts of ¹H and ¹⁹F. The chemical shift of ¹⁹F exhibited characteristics related to the density of CO₂,

Table 2 Factors affecting the solubility and viscosity of polymers in CO₂

| Factor | Solubility | Viscosity |
|-------------------|----------------------------|-----------|
| Concentration | Increase and then decrease | Increase |
| Molecular weight | Decrease | Increase |
| Chain flexibility | Increase | Decrease |
| Atactic structure | Increase | — |
| Branching degree | Increase | Increase |
| Side chain length | Decrease | Increase |
| Temperature | Decrease | Decrease |
| Pressure | Increase | Increase |
| Shear force | Increase | Decrease |



with a significant shift greater than that of ^1H . This difference originated from the van der Waals forces between the fluorine and CO_2 molecules. McHugh⁵⁰ compared the solubility of poly(vinyl difluoride-*co*-hexafluoropropylene) (fluorel) and poly(tetrafluoroethylene-*co*-hexafluoropropylene) (FEP19). It was found that fluorel could dissolve under conditions of 100 °C and 75 MPa, while FEP19, despite the introduction of fluorine-containing groups, lacked polar vinyl groups and tended to precipitate due to strong self-association. It was also observed in fluorinated polyisoprene that polar groups can enhance the interaction between the dipole moment and the quadrupole moment. These studies demonstrated that fluoropolymers are more soluble in CO_2 than other compounds containing weakly polar groups.⁵¹

McClain⁵² demonstrated that high-molecular-weight poly-fluoropropyl acrylate (PFOA) could also dissolve in CO_2 and increase the viscosity of the system. PFOA is known to be the polymer with the highest affinity for CO_2 . DeSimone^{53,54} reported that PFOA with a molecular weight of about 1 400 000 could increase the viscosity from 0.08 cp to 0.2–0.6 cp. Fluorinated polymers can cause environmental pollution, but polymers with fewer than seven fluorocarbons do not have bioaccumulative properties. Consequently, Lemaire⁵⁵ synthesized PFA with short fluorocarbon chains containing 4 and 6 fluorines, which had almost the same solubility and thickening effect as PFA with long fluorocarbon chains (C_8F_{17}) at temperatures between 25–125 °C. Zuberi⁴³ tested the phase behavior and oil displacement efficiency of PFA (Mw = 250 000) containing six fluorocarbons in CO_2 . Although PFA could dissolve well in CO_2 , it was not soluble in light hydrocarbons. This is very disadvantageous in the mobility-control process because CO_2 can extract light hydrocarbons from crude oil during the oil displacement process, and once the light hydrocarbons dissolve in CO_2 , they can cause the PFA to precipitate. Experiments proved that even at a pressure of 62 MPa, 1 wt% PFA could not dissolve in CO_2 containing 30 wt% of mixed light hydrocarbons ranging from C_6 to C_{20} . Using Berea sandstone and by injecting 2 PV of pure CO_2 and thickened CO_2 for comparison, the oil displacement efficiency was found to increase by 16%. Also, the pressure difference increased sharply by 8–9 times after injecting the thickened CO_2 , which was inconsistent with the viscosity test results showing a 3–4 times increase. The reason for the difference was the blockage of the pore throats caused by polymer precipitation.

Xu and Enick⁵⁶ synthesized a copolymer PolyFAST (Mw = 540 000) comprising 71% fluoroacrylate and 29% styrene. PolyFAST with a molecular weight of 540 000 had a solubility of 0.25–2 wt% under the conditions of 20 MPa and temperature between 298–373 K. They also found that a thickener concentration of just 1.5 wt% could increase the system's viscosity by 19 times.

Taking advantage of the high solubility of perfluoropolyether in CO_2 , Enick and Beckman⁵⁷ synthesized a fluorinated polyurethane disulfonate with a molecular weight of 32 500 and that could be mixed with CO_2 in any ratio under the conditions of 298 K and 20–34 MPa. Under 34.5 MPa, a thickener concentration of 4 wt% could increase the system viscosity by 2.7 times.

However, the high price of the fluorinated ether oil makes it costly to use as a thickener.

Enick⁵⁸ synthesized a random copolymer of poly(tetrafluoroethylene-vinyl acetate), and it was found that when the content of tetrafluoroethylene (TFE) reached 19 mol%, the polymer had the highest solubility in CO_2 . When the TFE content in the copolymer was 47 mol%, the solubility was lower than that of PVAc. Molecular dynamics simulation results indicated that when CO_2 molecules simultaneously interact with fluorine atoms and hydrogen bonds, the solubility of the copolymer was no longer enhanced by the binding of CO_2 to the fluorinated part. This was because the fluorinated units act as Lewis bases and the hydrogen-bonding parts act as Lewis acids during the binding process, leading to a change in the properties of the copolymer.

A. G. Goicochea⁵⁹ utilized dissipative particle dynamics to simulate the shear viscosity of styrene-fluoroacrylate (HFDA-STY), poly(1-decene) (P1D), and poly(vinyl ethyl ether) (PVEE) in CO_2 , and their results were within 6% of the experimental outcomes. The findings indicated that the linear PVEE formed a molecular association network, whereas P1D did not associate but rather adsorbed CO_2 due to its six branches, thus exhibiting higher solubility. HFDA primarily achieved the best thickening effect through the high affinity of fluorine for CO_2 and the π - π stacking between styrene rings, demonstrating a two orders higher magnitude of viscosity than the non-fluorinated solution (Fig. 2).

Dai^{61,62} synthesized a series of copolymers of heptadecafluorodecyl acrylate and styrene (HFDA-*co*-STY) with different monomer ratios. As the content of phenyl groups in the copolymer increased, both the solubility pressure and thickening ability of the copolymer increased.

Sun⁶³ synthesized a copolymer of vinyl benzoate and heptadecafluorodecyl acrylate, P(VBe-*co*-HFDA). Molecular dynamics simulations were used to characterize the solubility and thickening effects of the VBe content in the system, and the results were compared with those of the PHFDA homopolymer. The findings indicated that when the VBe content was 33%, the thickening effect was optimal. At a concentration of 5 wt%, the copolymer could increase the system's viscosity by 438 times, significantly higher than the thickening ability of the PHFDA homopolymer.

Kilic⁶⁴ investigated the effect of the structure of aromatic acrylate-fluoroacrylate copolymers on the viscosity of CO_2 , and

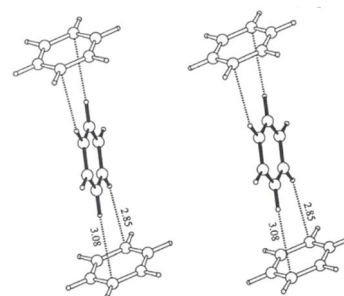


Fig. 2 π - π stacking between benzene rings.⁶⁰



found that these copolymers could dissolve in CO₂ at pressures below 15 MPa and a temperature of 295 K. The solution viscosity increased with the increasing content of aromatic acrylate units in the copolymer. However, beyond a certain content, the phenyl rings shifted from intermolecular association to intramolecular association, leading to a decrease in viscosity. Additionally, higher pressures were found to strengthen the intermolecular association. The experiments demonstrated that an optimal content of 29% aromatic acrylate resulted in the best thickening effect, achieving a dissolution pressure comparable to that of PolyFAST.

Huang⁶⁵ synthesized a copolymer of fluoroacrylate, styrene, and sulfonated styrene, which increased the solution viscosity through the association of sulfonated styrene. The results showed that this copolymer was less soluble than the non-sulfonated polymer, but the thickening effect was enhanced. The optimal content of styrene was 29%, which obtained the same result as for PolyFAST. The addition of 1–5 wt% copolymer increased the system's viscosity by 3–10 times at 25 °C and 34.48 MPa. Zhang⁶⁶ further optimized the ratio of copolymer monomers and found that under suitable solubility, a higher content of sulfonated styrene monomer could further enhance the thickening ability. The best ratio was ultimately determined to be 60% PHDA-24% PST-16% S.

Fluoropolymers do not significantly enhance the viscosity of CO₂, but fluorine-containing groups have good affinity with CO₂ and high solubility in it. By adding a small amount of fluorine-containing groups to polymers with strong self-association, the originally difficult-to-dissolve molecular chains or groups can become more stable in CO₂. The solute molecules can form a network structure in supercritical CO₂ without the need for co-solvents, achieving this through strong interactions, such as hydrogen bonding. Although fluoropolymers are costly and have certain biological hazards, their high affinity for CO₂, the absence of a need for co-solvents, and their low usage make them advantageous and promising for modification and copolymerization (Table 3).

3.2 Siloxane polymers

Siloxanes are excellent electron-donating groups that can bond with the electron-deficient carbon in CO₂. The high flexibility of siloxane chains also promotes the dissolution of molecules in CO₂. Siloxane polymers have long been widely applied in the field of CO₂ thickeners. Bae and Irani^{67,68} first discovered that polydimethylsiloxane (PDMS) with a molecular weight of 197 000 could dissolve in CO₂ and increase the system's viscosity to 1.2 cp, and it effectively delayed gas breakthrough in oil displacement experiments. Du⁶⁹ also conducted a series of experiments and simulation studies on a PDMS–toluene system as a fracturing fluid, which could thicken CO₂ by 40 times at 42 °C and 20 MPa. PDMS remains one of the most effective siloxanes CO₂ thickeners, but it requires a large amount of toluene as a co-solvent.

Zhao⁷⁰ studied the solubility and thickening properties of a series of PDMSs with different end groups. Hydroxyl-end capped PDMS, vinyl-end capped PDMS, and hydrogen-end

capped PDMS were compared respectively, and it was found that under the same intrinsic viscosity, the solubility pressure of vinyl-end capped PDMS was the lowest. Further, 8 wt% of 1000 cst vinyl-end capped PDMS achieved a system viscosity of 12.57 mPa s at 313.13 K. Using kerosene as a co-solvent, 5 wt% of 3000 cst vinyl-end capped PDMS and 2 wt% of kerosene achieved a system viscosity of 14.87 mPa s at 313 K and 39.6 MPa.

Enick⁵⁸ grafted various groups with good affinity for CO₂, such as carbonyl, ether, acetate, and trimethyl branched groups, onto siloxanes. The solubility of these groups in CO₂ at 295 K was then tested, and it was found that the optimal substitution degree for carbonyl groups was within 4–8%, for ethers it was 8%, and for esters it was 20%. Increasing the degree of substitution increased the solubility pressure, with complete substitution resulting in insolubility in CO₂. This was because the addition of side chains increases the rigidity of the molecular chain and the cohesive energy density, and when the substitution degree exceeds a certain critical point, the negative impact on solubility caused by these factors exceeds the Lewis acid–base interaction between the carbonyl group and CO₂ molecules. The solubility of trimethyl branched siloxanes was found to be almost the same as that of the PDMS, because the branched substitution increases the free volume of the molecule and enhances the flexibility of the molecular chain, compensating for the increase in cohesive energy density.

Li⁷¹ synthesized a siloxane copolymer for fracturing thickening, which could thicken CO₂ at 8–12 MPa by 4.1–5.7 times at temperatures between 35–55 °C, with 3 wt% of the copolymer and 7 wt% of the co-solvent toluene. The interaction between the N on the polymer side chain and the C in CO₂ increased the solubility, while the O on the siloxane main chain, the C–H bonds in toluene, and the C=O double bonds in CO₂ worked together to form a stable macromolecular network structure. The team also synthesized siloxane thickeners AOB, BTMT, and PDMS with epoxy groups as end groups. Comparing them with regular PDMS, AOB's thickening effect was 8 times that of PDMS at 310 K and 15 MPa.⁷² BTMT also showed better resistance to filtration than PDMS in fracturing experiments.⁷³ The solubility pressure of PDMS with epoxy end groups was less than 8 MPa. The thickening effect was 3–4 times higher than that of PDMS at the same molecular weight at temperatures between 20–50 °C.⁷⁴

O'Brien⁷⁵ synthesized a series of low-molecular-weight polysiloxanes with aromatic amide groups at the ends, and found that siloxanes with amide-anthraquinone (AQCA) at the ends had a certain thickening effect on CO₂ with the co-solvent hexane. A CO₂ solution containing 13.3 wt% of the thickener and 26.7 wt% of hexane demonstrated a viscosity 9 times that of the CO₂–hexane mixture at 25 °C and 20.7 MPa.

Liu⁷⁶ synthesized two siloxane-based thickeners for fracturing 1,3,5,7-tetramethyl cyclotetrasiloxane (HBD). The internally branched HBD-2 molecule was found to have a larger free volume and was more prone to self-association, thus having a better thickening effect than HBD-1. They also synthesized a series of HS polymers without a siloxane ring.⁷⁷ At 298 K and 7.48 MPa, all three thickeners dissolved after being left to stand for 12 h, without a cloud point. Possibly due to CO₂ thickening or incomplete dissolution, the solution remained translucent in



Table 3 Some of the fluoropolymers discussed in this paper

| Polymer | Structure | Co-solvent | Conditions | Solubility | Viscosity/cp | Reference |
|----------------|-----------|------------|-------------------|------------|--------------|--------------|
| PFA | | — | 50 °C | 6.7 wt% | 0.6 | 43 and 52–55 |
| PolyFAST | | — | 373 K 20 MPa | 1.5 wt% | 19 | 56 |
| HFDA-co-STY | | — | 35 °C 30 MPa | 5 wt% | 7.06 | 61 and 62 |
| P(VBe-co-HFDA) | | — | 308.2 K 30 MPa | 5 wt% | 8.76 | 63 |
| PEA-FA | | — | 295 K 41.4 MPa | 5 wt% | 2.55 | 64 |
| PHFDA-Pst-S | | — | 273 K 28 MPa | 1 wt% | 2.01 | 65 and 66 |

the reactor. HS-3 performed the best among the three thickeners, which contained more hydroxyl groups and longer side chains. It led to thickening by 151–163 times with the addition of 5 wt% polymer.

Gallo⁷⁸ utilized the CPCM solvation model and viscosity measurements to compare four different types of siloxane compounds and found that the solubility of polysiloxanes was about 20% higher than that of linear PDMS with similar molecular weights. The polar groups within silsesquioxane

molecules could promote solvation, while polar groups on the outer layer and ends of the molecules could lead to strong intermolecular interactions. A mixture of 6.9 wt% silsesquioxanes and nanoparticles with CO₂ reached a viscosity of 0.25 cp at 180 bar and 55 °C, showing it was more effective than linear PDMS and it also exhibited greater viscosity stability with temperature changes.

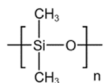
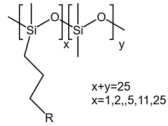
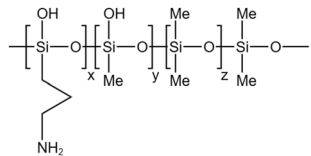
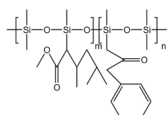
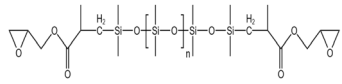
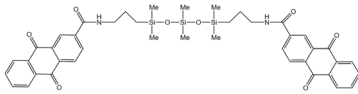
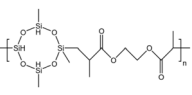
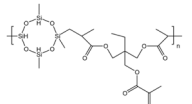
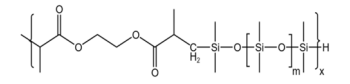
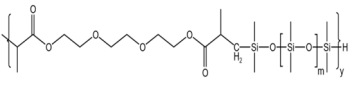
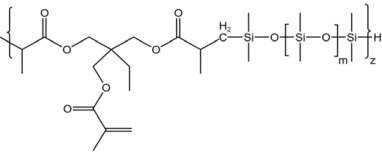
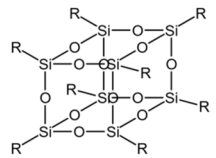
Siloxane polymers have a highly flexible backbone and strong affinity for CO₂, making them potentially effective CO₂



thickeners. However, siloxane compounds are expensive, and most research has focused on low-molecular-weight siloxanes that do not inherently possess thickening capabilities.

Typically, more than 10 wt% co-solvents are required to assist in thickening. In addition to searching for effective molecular structures, it is necessary to further investigate the thickening

Table 4 Some of the siloxane polymers discussed in this paper

| Polymer | Structure | Co-solvent | Conditions | Solubility | Viscosity/cp | Reference |
|---|---|-------------|---------------------|------------|--------------|-----------|
| PDMS |  | Toluene | 54.4 °C 17.2 MPa | 4 wt% | 1.2 | 67–69 |
| Grafted methylhydrosiloxane-dimethylsiloxane copolymers |  | — | 295 K 5–45 MPa | 1–5 wt% | — | 58 |
| Silicone ternary copolymer |  | Toluene | 55 °C 12 MPa | 3 wt% | 0.15 | 71 |
| AOB |  | Cyclohexane | 310 K 15 MPa | 3 wt% | 1.8 | 72 |
| Epoxy-terminated PDMS |  | Toluene | 303 K 14 MPa | 3 wt% | 0.9 | 74 |
| AQCA-PDMS |  | Hexane | 25 °C 20.7 MPa | 13.3 wt% | 0.86 | 75 |
| HBD-1 |  | — | 32.15 °C 10 MPa | 5 wt% | 3.5 | 76 |
| HBD-2 |  | — | 32.15 °C 10 MPa | 5 wt% | 4.48 | 76 |
| HS-1 |  | — | 16 MPa, 305 K | 5 wt% | 1.02 | 77 |
| HS-2 |  | — | 16 MPa, 305 K | 5 wt% | 2.78 | 77 |
| HS-3 |  | — | 16 MPa, 305 K | 5 wt% | 3.26 | 77 |
| Silsesquioxane |  | — | 180 bar, 55 °C | 6.9 wt% | 0.25 | 78 |



capabilities of high-molecular-weight siloxane polymers and the mechanisms of co-solvent-assisted thickening. Optimizing the system and selecting the appropriate molecular weight materials are key research focuses for siloxane thickeners (Table 4).

3.3 Hydrocarbon polymers

Due to the lack of highly polar groups in hydrocarbon polymers, their interactions with CO₂ molecules are mostly through Lewis acid–base interactions and hydrogen bonding.⁷⁹ Within the CO₂ molecule, the oxygen atoms have a higher electron density than the carbon atom, resulting in a significant charge separation, with the carbon atom bearing a positive charge, acting as a Lewis acid, and the oxygen atoms bearing a negative charge, acting as Lewis bases⁷⁹ (Fig. 3). The solubility of polymers in CO₂ can be enhanced by adding electron-donating groups, such as carbonyl, ether, sulfone, and ester, to the hydrocarbon polymers (Fig. 4), which strengthens the Lewis acid–base and hydrogen-bonding interactions with CO₂.⁸¹ The acetate group is an excellent electron-donating group, with poly(vinyl acetate) (PVAc) being one of the hydrocarbon polymers with the best solubility in CO₂, but its solubility is significantly lower than that of PDMS and PFOA.⁸²

Khanh⁸³ simulated the interaction between a series of hydrocarbons containing hydroxyl, carbonyl, sulfone, carboxyl, and amide groups with CO₂ molecules. The results showed that the stability of the complexes formed by carbonyl and sulfone groups with CO₂ was stronger than that of other groups, and the benzene ring also had a certain promoting effect on the stability of the system. It was proven that the stability of the complex was mainly determined by the Lewis acid–base interactions and hydrogen bonding. Apart from the interaction between the carboxyl group and CO₂, which was mainly derived from hydrogen bonding, the interaction between other groups and CO₂ was mainly determined by the Lewis acid–base interactions.

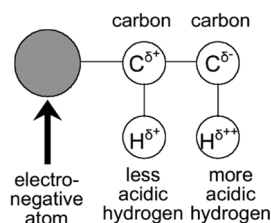


Fig. 3 Effect of a highly electronegative atom on charge distribution in a molecule.⁸⁰

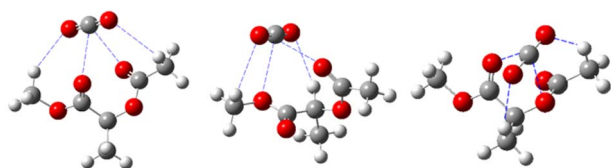


Fig. 4 Hydrogen bonding and Lewis acid–base interactions between CO₂ and polymers.⁶⁰

Polypropylene oxide (PPO) with a molecular weight less than 2000 is more soluble in CO₂ than poly(vinyl acetate) (PVAc), but its solubility significantly decreases at higher molecular weights. Therefore, Enick⁵⁸ attempted to modify PPO by grafting with methyl ether, but this did not increase the solubility. They also investigated the effects of hydroxyl and acetate end groups on PPO and found that only the acetate-terminated PPO showed a decrease in dissolution pressure, by 3.4–6.9 MPa at 295 K. The hydrogen bonds formed by hydroxyl groups increased the intermolecular interactions, reducing the solubility. Then they discovered that low concentrations of poly(ethylene vinyl ether) (PEVE) had nearly the same dissolution pressure as PVAc. Subsequently, Lee⁸⁴ demonstrated that low-molecular-weight PEVE could dissolve in CO₂ but did not exhibit a significant thickening ability.

Xue⁴⁵ simulated a random copolymer of poly(vinyl acetate–vinyl ether) PVAEE. Under conditions of 308 K and a CO₂ density of 0.854 g cm⁻³, the simulated viscosity of scCO₂ was reported to be 0.1268 cp. When the PVAEE content was 1.19 wt% and 2.35 wt%, the viscosity of the system reached 0.2037 cp and 0.4135 cp, respectively showing increases of 2–3 times. They compared the binding energy and dissociation energy of ester groups and ether bonds and found that ester groups could bind more easily to CO₂ molecules than ether bonds.

Hu⁸⁵ synthesized P(VAc-co-VEE) using vinyl acetate (VAc) and vinyl ethyl ether (VEE) groups and found that the random copolymer containing 30% VEE had the highest affinity for CO₂. The VEE monomer could also reduce the interactions between polymers.

Wang⁸⁰ designed a series of polymers, comprising OAO, PVMME, and PVMEE. OAO could dissolve up to 5 wt% at 298 K and 25 MPa, and PVMME could dissolve up to 3 wt% at 120 MPa. Under the same conditions, the solubility of PVMME in CO₂ was lower than that of PVAc but better than that of PLA and PMA, because the ether oxygen in the main chain of PVMME had a higher affinity for CO₂ than the carbonyl group in PMA.

Heller⁸⁶ tested several commercially available hydrocarbon polymers soluble in hexane/ethanol, predicting their solubility behavior in CO₂ by measuring their solubility in butane. It was ultimately found that poly- α -olefins (P1D) and atactic polybutene had the highest solubility, but subsequent research proved that only P-1-D had a very low solubility in CO₂.

Tapriyal⁶⁰ synthesized a non-fluorinated analog of PolyFAST, PolyBOVA, using vinyl acetate and a monomer with a rigid benzene ring side group. PolyBOVA with 5% benzoyl groups could dissolve up to 3 wt% at 298 K with a pressure of 64 MPa required, while it was insoluble in CO₂ with 10% benzoyl groups. The viscosity of solutions with 1 wt% and 2 wt% PolyBOVA increased by only 40% and 80%, respectively.

Zhang⁸⁷ synthesized a polyether-type carbon–hydrogen thickener, poly(ethylene oxide-co-propylene oxide) (PPOGPEAc), and compared it with the non-substituted polymer PPOAc. Under 36.3% PPOGPEAc, the viscosity of the system reached 0.35 mPa s, which was 2.3 times the thickening effect of PPOAc. The copolymer showed the best thickening effect when the phenyl content was 36.3 mol%. It was also found that adding



more phenyl groups would increase the intramolecular interactions, affecting the intermolecular associations and reducing the system's solubility.

Raveendran and Wallen⁸⁸ tested a series of acetylated carbohydrate substances for their solubility in CO₂. The large number of hydrogen bonds and Lewis acid–base interactions formed by the carbonyl groups within the sugar molecules made them highly soluble in CO₂. Potluri⁸⁹ found that the higher the content of sugar molecules, the greater the solubility pressure. Cyclodextrin had a cloud point pressure of 25–45 MPa at concentrations of 5–30 wt% at 313 K.

Tapriyal⁹⁰ synthesized a polymer, PACGIcVE, with a polyethylene main chain and side chains containing acetylated sugar groups, and compared it with several amorphous polylactic acids (PLAs) with different end groups.⁹¹ PLA with end groups containing two ether bonds showed better results than PLA with end groups containing two ether bonds and branched side chains, indicating that linear ether oxygen bonds are more conducive to solubility. The solubility pressure of PACGIcVE with a molecular weight of 40 000 was 65–75 MPa, much lower than that of PLA, but 10–20 MPa higher than that of PVAc.

Due to environmental concerns over fluoropolymers and the high cost of siloxane polymers, which often require large amounts of co-solvents for viscosity enhancement, the development of hydrocarbon polymer thickeners for CO₂ is a current research focus. However, hydrocarbon groups do not have a high affinity for CO₂, and can only form a stable network structure within the solution through modification of the molecular structure to create Lewis acid–base interactions with CO₂, resulting in a solution that is less viscous compared to fluorinated and siloxane polymers (Table 5).

3.4 Small molecular compounds

Small molecule compounds have greater solubility and can form rod-like, worm-like, or helical micelles in CO₂ through associative interactions, making them potential alternatives to high-molecular-weight polymer thickeners. Similarly, these compounds also need to have a CO₂-philic group, which enhances the solubility and a CO₂-phobic group, which promotes intermolecular association.

Amine-based compounds are considered to have a certain solubility in CO₂ due to their weak self-association and low glass transition temperatures, as well as having a cohesive energy density similar to that of siloxanes. Enick⁵⁸ tested polyvinylethyleneamine (PPEI) and a series of carbonyl-modified compounds, including PMAEI, PEO, and PDMAA. These compounds showed good miscibility with CO₂ in molecular dynamics simulations. However, the experimental results indicated that PPEI, PMAEI, and PEO were insoluble in CO₂ under a high pressure of 45 MPa. Here, the interaction forces between the C atoms and N atoms could not overcome the self-association of amine groups, despite the addition of carbonyl groups. Nevertheless, 0.7 wt% PDMAA swelled in CO₂ at 45 MPa, indicating that the N atom, acting as an electron-donating group, enhanced the Lewis acid–base interaction between the carbonyl group and CO₂.

J. P. Heller⁹² found that compounds centered on Sn atoms with three butyl arms and fluorine atoms could increase the viscosity of light hydrocarbons by three orders of magnitude at a low concentration of 1 wt%. Here, the butyl arms could extend into the alkanes to enhance the solubility, while the positively charged Sn atoms could take part in linear associative interactions with the negatively charged F atoms in neighboring molecules. The butyl arms could promote the stability of this associative structure, but these compounds were not soluble in CO₂. Therefore, Shi⁹³ synthesized a series of fluorostannanes with three fluoroalkyl arms, among which only the semi-fluorinated hexylfluorostannane increased the viscosity, by 2–3 times. The reason for the relatively low viscosity enhancement is that the fluorine atoms on the semi-fluorinated arms competed with the fluorine atoms bonded to the Sn atoms, disrupting the linear associative structure.

Research has shown that hydroxyl aluminum disoaps can thicken light hydrocarbons, with the ester chains at the molecular ends helping to form cylindrical micelles that can connect with each other, while the straight-chain ends do not have thickening ability. Enick⁹⁴ attempted to synthesize a series of hydroxyl aluminum disoaps, modifying the end chains to fluorinated chains or branched alkyl chains, but none were soluble in CO₂.

12-Hydroxystearic acid (HSA) is considered to be a potential CO₂ thickener due to its ability to gel light hydrocarbons,⁹⁵ However, it is only soluble in CO₂ when ethanol is added as a co-solvent. A solution with 3 wt% HSA and 15 wt% ethanol could increase the viscosity of CO₂ by 100 times at 28 °C and 12.4 MPa. HSA undergoes a gelation reaction when heated and dissolved in CO₂ and then cooled. Hydrogen bonding causes the molecular chains to stack together, forming a fibrous network gel with a high porosity after the solution cools. However, this type of gel can adhere to the rock surface in porous media, making HSA unsuitable for the EOR process.

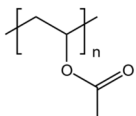
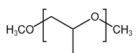
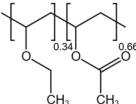
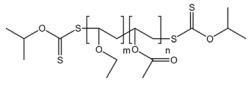
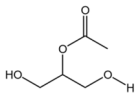
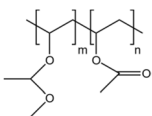
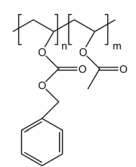
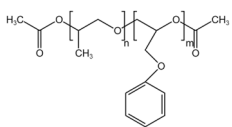
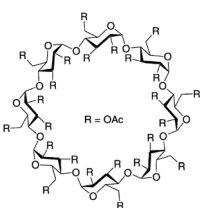
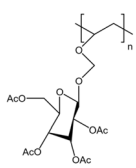
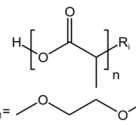
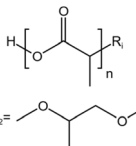
Zhou⁹⁶ synthesized a fluorine-containing urea-based tetra-arm oligomer, BPFAUH. After reaching a concentration of 2%, the viscosity of the system increased only slightly, because the formation and rupture of hydrogen bonds reached equilibrium during the formation of the network structure.

Tapriyal⁶⁰ synthesized a series of self-assembling compounds containing urea and acetate groups derived from acetylated sugars. The carbonyl oxygen in the urea group could form hydrogen bonds with hydrogen atoms, linking molecules to form a two-dimensional sheet-like structure. A bis-arm compound containing one bis-urea and two acetylated sugars displayed much lower solubility compared to a dendritic compound containing one bis-urea and four acetylated sugars under the same conditions.

Doherty⁹⁷ synthesized three categories of small molecule compounds with amide or urea groups and a siloxane main chain: amide compounds, amides with benzene rings, and ureas with benzene rings. Their experiments showed that compounds containing urea groups were superior to amides and esters in thickening. Highly branched molecules dissolved more easily than linear ones. However, the thickening effect was achieved by adding a large amount of co-solvents. Molecules



Table 5 Some of the hydrocarbon polymers discussed in this paper

| Polymer | Structure | Co-solvent | Conditions | Solubility | Viscosity/cp | Reference |
|---------------------------------|---|------------|------------------|------------|--------------|-----------|
| PVAc |  | — | 308 K, 30.31 MPa | 0.05 wt% | — | 82 |
| PPO |  | — | 295 K, 35 MPa | 3.5 wt% | — | 58 |
| PVAEE |  | — | 308 K, 18.5 MPa | 2.35 wt% | 0.4135 | 45 |
| P(VAc-co-VEE) |  | — | 35 °C, 24 MPa | 0.2 wt% | — | 85 |
| OAO |  | — | 298 K, 25 MPa | 5 wt% | — | 80 |
| PVMME |  | — | 298 K, 120 MPa | 3 wt% | — | 80 |
| PolyBOVA |  | — | 298 K, 64 MPa | 2 wt% | 0.27 | 60 |
| PPOGPEAc |  | — | 30 °C, 35 MPa | 36.3% | 0.35 | 87 |
| Peracetylated sugar derivatives |  | — | 313 K, 45 MPa | 30 wt% | — | 88 and 89 |
| PAcGIcVE |  | — | 298 K, 52 MPa | 5 wt% | — | 90 |
| PLA |  | — | 298 K, 50 MPa | 5 wt% | — | 91 |
| PLA |  | — | 298 K, 60 MPa | 3 wt% | — | 91 |

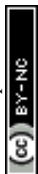
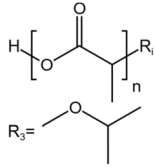


Table 5 (Contd.)

| Polymer | Structure | Co-solvent | Conditions | Solubility | Viscosity/cp | Reference |
|---------|---|------------|----------------|------------|--------------|-----------|
| PLA |  | — | 298 K, 120 MPa | 5 wt% | — | 91 |

centered around benzene triurea had very little self-interaction and could not form sheet-like networks or long linear structures.

Small molecular thickeners have shown great potential for viscosity enhancement. Some research has aimed to enhance the solubility and viscosity of CO₂ by incorporating nitrogen-containing groups (such as amine and urea groups) that can form weak interactions between N–N atoms and strong interactions between N–C atoms. Extensive experiments have proven that nitrogen-containing groups strengthen the interaction between other CO₂-philic groups within the thickener and CO₂ molecules, which helps to some extent in the dissolution of polymers in CO₂. The weak interactions between N atoms also contribute to the increase in system viscosity. However, these groups only have a certain effect when added to other molecules with good solubility and they are not effective enough to be the main functional groups. Nevertheless, the advantage of forming a significant increase in system viscosity by combining with highly CO₂-philic groups still give them a certain application potential (Table 6).

3.5 Nanoparticles

Nanomaterials have been applied in various industries for various purposes, such as electrocatalytic CO₂ reduction, catalytic conversion of CO₂, and the adsorption of CO₂ by functionalized composite materials.^{98–100} Nanoparticles have a high specific surface area, which provides an excellent driving force for diffusion.¹⁰¹ They can travel long distances through the pore channels within the reservoir, interact with the injected fluids, and thus affect the fluid flow characteristics deep within the reservoir.¹⁰² Researchers have investigated the relationship between nanomaterials and CO₂ across several domains, including the capture of CO₂ through carbon nanotubes and the utilization of nanosilica for enhancing CO₂ storage within geological formations.^{103,104} Introducing nanoparticles in the CO₂ EOR process can not only alter certain properties, such as the viscosity, density, thermal conductivity, and interfacial tension, of the displacement fluid but also change the reservoir properties, such as the wettability of rock surfaces. The mechanisms of nanomaterials can be divided into two categories in the process of mobility control: first, by stabilizing CO₂ foams that are prone to degradation due to rock adsorption and high reservoir temperatures by adsorbing at the two-phase interface;

and second, by forming a stable suspension of metal or polymer nanoparticles in CO₂ to thicken the fluid.¹⁰⁵ The addition of nanoparticles has been proven to be an effective means of mobility control, with studies demonstrating that alternating the injection of thickened CO₂ nanofluids and CO₂ can achieve higher sweep efficiency.^{106,107}

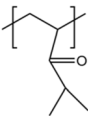
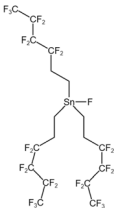
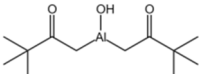
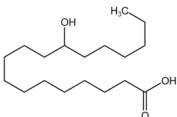
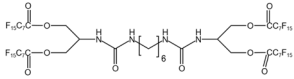
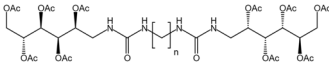
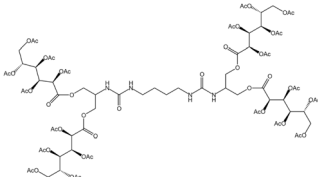
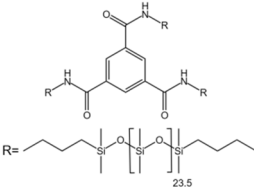
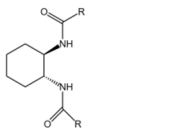
However, the spatial repulsive forces between nanoparticles cannot offset the attractive van der Waals forces, making them prone to flocculation and difficult to stably disperse in CO₂. Therefore, it is often necessary to modify the nanoparticles with CO₂-philic groups to enhance their stability in solution. There are various types of nanoparticles, including polymer nanoparticles, metal nanoparticles, carbon-based nanoparticles, silicon-based nanoparticles, and Janus nanoparticles, among which SiO₂ nanoparticles have been proven to have good thickening effects on displacement fluids.¹⁰⁸ Dickson¹⁰⁹ modified SiO₂ particles with fluoroalkyl ethoxy silane, resulting in a polymer shell that formed a core-shell structure around the particles. This modification allowed SiO₂ particles, which were previously insoluble in CO₂, to remain stable for up to 30 min at 25 °C and 34 MPa. Visintin¹¹⁰ grafted fluoroalkyl chains onto silica and alumina particles, enabling them to be stably dispersed in CO₂. Bell¹¹¹ used isostearic acid as a ligand to promote the dispersion of silver nanoparticles in CO₂, forming a stable solution at 295 K and 13.8 MPa.

Yates¹¹² investigated the effect of the co-solvent hexane on the dispersion of nanoparticles. Similar to the mechanism of polymers dissolving in CO₂, nanoparticles could only be stably dispersed when the density of CO₂ reached a critical level. The experiment proved that the system could stably exist after adding SiO₂ nanoparticles grafted with PDMS and 15 wt% hexane to CO₂. The addition of hexane enhanced the interaction between the PDMS side chains and CO₂, increasing the number of chains extending into the solvent and weakening the inter-chain interactions.

Xu¹¹³ prepared a type of fluoropolymer-modified nanoparticles for tracing and evaluating CO₂ sequestration. These particles did not adsorb on the formation surface and aggregate. The polymer, which contained fluorocarbon, carbonyl oxygen, and benzene rings, was grafted onto Fe₃O₄ and SiO₂ nanoparticles with a diameter of less than 50 nm, increasing their affinity with CO₂. The polymer grafting density on the surface of Fe₃O₄ nanoparticles was higher. It dissolved at 34.5 °



Table 6 Some of the small molecular compounds discussed in this paper

| Polymer | Structure | Co-solvent | Conditions | Solubility | Viscosity/cp | Reference |
|---|---|------------|------------------|------------|--------------|-----------|
| PDMAA |  | — | 298 K, 45 MPa | 0.7 wt% | — | 58 |
| Tri (semi-fluorinated hexyl tin fluoride) |  | — | 297 K, 16.5 MPa | 4 wt% | 0.27 | 93 |
| Hydroxy aluminum disoap |  | — | — | Insoluble | — | 94 |
| 12-HAS |  | Ethanol | 28 °C, 12.4 MPa | 3 wt% | 7.6 | 95 |
| BPFAUH |  | — | 313.13 K, 19 MPa | 3 wt% | 19.2 | 96 |
| Bis-urea polymer |  | — | 298 K, 65 MPa | 5 wt% | — | 60 |
| Bis-urea polymer |  | — | 298 K, 65 MPa | 1 wt% | — | 60 |
| Benzene trisurea polymer |  | Toluene | 25 °C, 5000 psi | 1.5 wt% | 3 | 97 |
| <i>trans</i> -1,2 Cyclohexanedicarboxamides |  | Toluene | 25 °C, 1500 psi | 1.6 wt% | 30 | 97 |

C and 16.1 MPa, while SiO₂ nanoparticles dissolved at 51 °C and 28.3 MPa.

Zhang¹¹⁴ synthesized a copolymer of fluorinated and sulfonated styrene for fracture thickening. Their experiments proved that 1 wt% of the copolymer could increase the viscosity by 100 times at 333 K and 28 MPa. On this basis, a type of polyester fiber nanoparticle was introduced, and the results

showed that this type of nanoparticle had good dispersion in the fluid. At 263 K, 28 MPa, and 5000 s⁻¹, the addition of 0.5 wt% of the nanoparticles could reduce the internal friction by 17%. The system is suitable for the fracturing process, but its ability to pass through core pores is still under investigation.

Khaledialidusti¹¹⁵ used molecular dynamics simulation to investigate the rheological properties of a scCO₂-CuO



nanoparticle system. They reported that 1 wt% of CuO nanoparticles increased the viscosity of the system by 1.3–2.5 times within the temperature range of 350–410 K at 20 MPa. Su¹¹⁶ conducted a stability analysis of a hydroxylated carbon nanotube (MWCNTs)–scCO₂ system. Their results indicated that as the volume concentration and temperature decreased, the stability of the nanofluid continuously improved. The system essentially reached a stable state after 4 min of circulating flow, while the sedimentation density continuously decreased with increasing the volume concentration and circulation flow time.

Wang¹¹⁷ added five types of nanoparticles, namely Cu-BTC, SiO₂, MCC, MWCNTs, and TiO₂, to the thickener HBD-2 and studied their synergistic effect on the fracturing system. It was found that only the addition of SiO₂ could significantly increase the apparent viscosity. A system containing 1 wt% SiO₂ nanoparticles and 5 wt% HBD-2 thickener was approximately 1.2–1.7 times more viscous than a system containing pure thickener under the conditions of 305–325 K and 10 MPa. The RDF results proved that the surface energy effect of SiO₂ could effectively promote the crosslinking between the polymer molecular chains.

Gandomkar¹¹⁸ synthesized a graphene oxide (GO)/P-1-D nanocomposite polymer, and the results showed that as the content of GO nanoparticles increased, the polymer's dissolution pressure continuously decreased, with the highest dissolution pressure at 100 °C being 24.1 MPa. Compared with pure P-1-D, GO/P-1-D could increase the system's viscosity by more than 5 times, but this thickening system was only tested in light hydrocarbon gases, not CO₂.

4. Application of CO₂ direct thickeners

CO₂-thickening systems are widely used in fracture and EOR processes. Due to the strong heterogeneity, low porosity, and low permeability of unconventional oil and gas reservoirs, it is necessary to rely on reservoir fracturing techniques to further exploit them. Traditional water-based fracturing has certain issues, such as high water consumption and environmental pollution.¹¹⁹ ScCO₂ has been used as a fracturing fluid since the 1960s. Compared to water-based fracturing, supercritical CO₂ fracturing has the advantages of a higher fracture strength and lower fracture pressure, and it does not clog pores, making it more suitable for the development of unconventional shale oil reservoirs.¹²⁰ However, CO₂ has a low viscosity and poor sand-carrying capacity, which hinders its field application. Adding thickeners to the system to increase the viscosity of CO₂ can greatly enhance the effectiveness of CO₂ fracturing.

Because of the different application scenarios, the requirements for thickeners in CO₂ EOR and CO₂ fracturing are different. In fracturing experiments, the adsorption amount of thickeners in the formation, shear resistance, and thickening multiple are key to evaluation, as sand-carrying has higher viscosity requirements. Siloxane polymers are commonly used as thickeners in fracturing, while adding silicate or metal nanoparticles can further assist in thickening. To achieve the

desired fracturing effect, a significant amount of thickener is required. Similarly, the CO₂ EOR process requires great attention to the cost and environmental friendliness of thickeners. EOR requires the thickening system to continuously pass through small pores and maintain displacement pressure, while also considering the temperature and pressure resistance of the thickener and its adsorption properties in the formation. Small molecule thickeners and environmentally friendly hydrocarbon polymers have more application potential in the EOR process.

In practical applications, CO₂ direct thickeners face numerous challenges. First, the common polymers available on the market are difficult to dissolve in CO₂, and the synthesis process of the thickeners is often complex. The need to add a significant amount of co-solvents leads to higher industrial costs. Second, thickeners tend to adsorb significantly within the formation, especially after coming into contact with oil and water. When the formation conditions are not sufficient to maintain the CO₂ thickening system as a stable single phase or at the critical point of a mixed phase, the solute can easily precipitate during flow. Moreover, CO₂ can mix with crude oil, and further reactions can occur between the polymer and substances in the crude oil. Although these reactions are mostly detrimental to the dissolution of the polymers in CO₂, they can also have certain positive effects. For example, adding PVAc and limonene to scCO₂ can prevent the flocculation of non-hydrogen-bonding asphaltenes.¹²¹ Considering the current research, while ensuring that functional groups have a high affinity for CO₂, the issue of adsorption also needs to be considered. Merely modifying the polymer at the molecular level makes it difficult to further improve the solubility of the polymer. Therefore, optimizing the system is the key to research on CO₂ direct thickeners. The polymer modification approach should not be limited to its interactions with CO₂; it is also necessary to consider changes in phase behavior after adding other auxiliary thickeners, such as nanoparticles. It is challenging for nanoparticles to achieve a stable dispersed state in CO₂; however, if they are added to the CO₂–polymer system and the affinity between the polymer and nanoparticles is increased, this can facilitate the uniform dispersion of nanoparticles while also enhancing the viscosity of the CO₂ solution. In porous media, nanoparticles preferentially adsorb onto the formation surface, and polymer thickeners can still play a role in increasing viscosity. Based on these challenges, there are currently no field experiment reports on CO₂ direct thickeners, and more convincing laboratory experiments are needed to substantiate their effectiveness.

5. Conclusion and outlook

Supercritical CO₂ direct thickeners have significant importance for CO₂ fracturing and CO₂ EOR. The development of thickeners is still mainly at the laboratory research stage, which includes ongoing work on their synthesis, structural characterization, solubility and thickening tests, and exploration of their working mechanisms. Due to high costs and other reasons, there are currently no reports on field applications. Therefore, developing



a low-cost, green thickener from a molecular perspective remains the primary research goal in the field of direct CO₂ thickeners.

In the system, hydrocarbon polymers lack highly polar groups and have poor affinity with CO₂, resulting in much lower solubility compared to fluoropolymers and siloxane polymers. The dissolution and thickening effects need to be optimized by modifying the hydrocarbon thickeners. Fluoropolymers are limited by pollution issues and are difficult to widely apply, but fluorine-containing groups have good affinity with CO₂ and high solubility in it. Adding a small amount of fluorine-containing groups to polymers with strong self-association can make the originally difficult-to-dissolve molecular chains or groups more stable in CO₂. High-molecular-weight siloxane polymers have poor solubility in CO₂, while low-molecular weight siloxanes lack a thickening ability. However, the addition of siloxane chain segments can promote the dissolution of compounds in CO₂ and so siloxanes are important materials for modifying hydrocarbon thickeners. For small molecule compounds that are more easily soluble, adjusting the intermolecular interaction forces and forming a stable network structure through intermolecular crosslinking is a key research focus. As research progresses, the addition of nanoparticles has brought new possibilities to the study of thickening agent systems. Nanoparticles can be modified themselves to have similar effects as surfactants, and can also change the properties of the displacing fluid through high surface energy and other microscopic effects. The addition of nanoparticles in CO₂-polymer solutions can not only enhance the thickening effect but also reduce the adsorption of polymers onto formations, making it an important research direction worthy of attention. Further studies are needed to understand the mechanisms and factors influencing the uniform dispersion of nanoparticles in the solution, how to strengthen the interaction between the nanoparticles and polymers through modification, and whether the synergistic effect of nanoparticles and polymers can reduce adsorption in porous media.

In characterization methods, most of the characterization techniques for CO₂ thickeners are still focused on compound synthesis, phase behavior, solubility pressure, viscosity characterization, and molecular dynamics simulation. The exploration of dissolution mechanisms and solvation patterns is not yet in-depth. It is necessary to start from microscopic factors, such as density, molecular weight, and polymer groups, and combine experiments and simulations to gradually explore the critical points and patterns of the morphological changes in CO₂. Characterization often requires high-temperature and high-pressure environments, and the experimental conditions are harsh. There is a need to develop a set of faster, simpler, and standardized characterization methods. The morphological changes of the molecular chains in CO₂ can refer to the theoretical studies of polymer chains in dilute solutions, using liquid solvents with solubility parameters close to that of CO₂ to replace the CO₂ gas, in order to determine the critical association concentration of the molecular chains. Semi-empirical regression equations can then be fitted based on experimental data.

In application, further research is needed on the mechanism of action of CO₂ thickening systems. CO₂, polymers, and oil-water phases react upon contact in formations, affecting the stability of a single system. Fluoropolymers can precipitate due to repulsive interactions with light hydrocarbons dissolved in CO₂, and siloxane polymers can also interact with hydroxyl groups in water molecules. Current displacement experiments have shown that CO₂ thickening systems can increase fluid viscosity, thereby increasing displacement pressure and enhancing the oil-recovery rates. However, after phase mixing internally, the main reason for the increased displacement pressure is likely not the increase in fluid viscosity but the precipitation of polymers causing plugging in the pores. Therefore, visualized microscopic displacement experiments are needed to demonstrate the mechanisms of action in the system.

Data Availability

Data sharing is not applicable to this article as no datasets were generated or analysed during the current study.

Conflicts of interest

There are no conflicts to declare.

Acknowledgements

The authors are grateful to the State Key Laboratory of Enhanced Oil and Gas Recovery of the Research Institute of Petroleum Exploration and Development for providing their support.

References

- 1 L. Shilun, Y. Tang and H. Chengxi, *Reservoir Evaluation and Development*, 2019, **9**, 1–8.
- 2 X. Teng, Synthesis and performance evaluation of supercritical carbon dioxide green thickener, Master's thesis, Beijing University of Chemical Technology, 2023, pp. 12–18.
- 3 R. Balch and B. McPherson, in *All Days, SPE*, Anchorage, Alaska, USA, 2016, p. SPE-180408-MS.
- 4 Y. Hu, M. Hao, G. Chen, R. Sun and S. Li, *Pet. Explor. Dev.*, 2019, **46**, 753–766.
- 5 D. Merchant, in *All Days, CMTC*, Houston, Texas, USA, 2017, p. CMTC-502866-MS.
- 6 J. Qin, H. Han and X. Liu, *Pet. Explor. Dev.*, 2015, **42**, 232–240.
- 7 H. Guo, J. Dong, Z. Wang, H. Liu, R. Ma, D. Kong, F. Wang, X. Xin, Y. Li and H. She, *OnePetro*, 2018, SPE-190286-MS.
- 8 C. Meng, Z. Yang and Z. Ming, *Pet. Sci. Technol.*, 2023, **42**, 49–56.
- 9 W. Qian, Research on the characteristics of CO₂ displacement and storage during supercritical CO₂ injection in low permeability reservoirs, Doctoral



- dissertation, China University of Petroleum, Beijing, 2022, pp. 25–29.
- 10 O. Massarweh and A. S. Abushaikh, *Petroleum*, 2022, **8**, 291–317.
 - 11 H. F. Al-Riyami, F. Kamali and F. Hussain, in *Day 3 Wed, April 26, 2017, SPE*, Dammam, Saudi Arabia, 2017, p. D033S046R006.
 - 12 H. Yongmao, W. Zenggui, J. Binshan, C. Yueming, L. Xiangjie and X. Petro, *OnePetro*, 2004, SPE 88883.
 - 13 P. Nikolai, B. Rabiya, A. Aslan and A. Ilmutdin, *J. Therm. Sci.*, 2019, **28**, 394–430.
 - 14 K. Trickett, D. Xing, R. Enick, J. Eastoe, M. J. Hollamby, K. J. Mutch, S. E. Rogers, R. K. Heenan and D. C. Steytler, *Langmuir*, 2010, **26**, 83–88.
 - 15 J. Han, M. Lee, W. Lee, Y. Lee and W. Sung, *Appl. Energy*, 2016, **161**, 85–91.
 - 16 Z. Wang, S. Yang, H. Lei, M. Yang, L. Li and S. Yang, *J. Pet. Sci. Eng.*, 2017, **150**, 376–385.
 - 17 S. Afzali, N. Rezaei and S. Zendejboudi, *Fuel*, 2018, **227**, 218–246.
 - 18 B. Brattækås and R. Seright, *SPE J.*, 2023, 1–17.
 - 19 G. Ren, H. Zhang and Q. P. Nguyen, *SPE J.*, 2013, **18**, 752–765.
 - 20 E. Luo, Y. Hu, B. Zhu, J. Wang and Z. Wang, *Oilfield Chem.*, 2013, **30**, 613–619.
 - 21 S. Kumar and A. Mandal, *J. Pet. Sci. Eng.*, 2017, **157**, 696–715.
 - 22 X. Li, S. Wang, B. Yuan and S. Chen, in *Day 4 Tue, April 17, 2018, SPE*, Tulsa, Oklahoma, USA, 2018, p. D041S017R006.
 - 23 J. R. Christensen, E. H. Stenby and A. Skauge, *SPE Reserv. Eval. Eng.*, 2001, **4**, 97–106.
 - 24 D. L. Tiffin and W. F. Yellig, *Soc. Pet. Eng. J.*, 1983, **23**, 447–455.
 - 25 J.-G. J. Shyeh-Yung, *OnePetro*, 1991, SPE-22651-MS.
 - 26 J. D. Rogers and R. B. Grigg, in *All Days, SPE*, Tulsa, Oklahoma, 2000, p. SPE-59329-MS.
 - 27 A. Valeev and A. Shevelev, in *Day 3 Wed, October 18, 2017, SPE*, Moscow, Russia, 2017, p. D033S030R001.
 - 28 X. Xu, A. Saeedi, Y. Zhang and K. Liu, in *Day 2 Wed, March 23, 2016, OTC*, Kuala Lumpur, Malaysia, 2016, p. D022S001R005.
 - 29 M. A. Almobarky, Z. A. Yousef and D. Schechter, *OnePetro*, 2017, CMTC-486486-MS.
 - 30 J. P. Heller, C. L. Lien and M. S. Kuntamukkula, *Soc. Pet. Eng. J.*, 1985, **25**, 603–613.
 - 31 D. Xing, B. Wei, K. Trickett, A. Mohamed, J. Eastoe, Y. Soong and R. Enick, in *All Days, SPE*, Tulsa, Oklahoma, USA, 2010, p. SPE-129907-MS.
 - 32 S. H. Raza, *Soc. Pet. Eng. J.*, 1970, **10**, 328–336.
 - 33 J. O. Alvarez, I. W. Saputra and D. S. Schechter, *SPE J.*, 2018, **23**, 2103–2117.
 - 34 E. Mayoral, J. A. Arcos-Casarrubias and A. Gama Goicochea, *Colloids Surf., A*, 2021, **615**, 126244.
 - 35 S. Liang, W. Luo, Z. Luo, W. Wang, X. Xue and B. Dong, *Molecules*, 2023, **28**, 8042.
 - 36 Z. Liu, P. Wei, Y. Qi, X. Huang and Y. Xie, *Carbohydr. Polym.*, 2023, **311**, 120759.
 - 37 F. Friedmann, T. L. Hughes, M. E. Smith, G. P. Hild, A. Wilson and S. N. Davies, *SPE Reserv. Eval. Eng.*, 1999, **2**, 4–13.
 - 38 W.-L. Kang, B.-B. Zhou, M. Issakhov and M. Gabdullin, *Pet. Sci.*, 2022, **19**, 1622–1640.
 - 39 B. Brattækås, R. Seright and G. Ersland, *SPE Prod. Oper.*, 2020, **35**, 202–213.
 - 40 Z. Wang, B. Bai, Y. Long and L. Wang, *SPE J.*, 2019, **24**, 2398–2408.
 - 41 N. Li, H. Zhang, X. Ren, J. Wang, J. Yu, C. Jiang, H. Zhang and Y. Li, *Gas Sci. Eng.*, 2024, **125**, 205312.
 - 42 X. Sun, Y. Zhang, G. Chen and Z. Gai, *Energies*, 2017, **10**, 345.
 - 43 H. Zakeri, Core flooding study of CO₂-soluble polymers for improved mobility control and conformance control, Master's thesis, University of Tulsa, 2011, pp. 28–32.
 - 44 P. Raffa, A. A. Broekhuis and F. Picchioni, *J. Pet. Sci. Eng.*, 2016, **145**, 723–733.
 - 45 P. Xue, J. Shi, X. Cao and S. Yuan, *Chem. Phys. Lett.*, 2018, **706**, 658–664.
 - 46 J. P. Heller, D. K. Dandge, R. J. Card and L. G. Donaruma, *Soc. Pet. Eng. J.*, 1985, **25**, 679–686.
 - 47 C. Lepilleur, E. J. Beckman, H. Schonemann and V. J. Krukoni, *Fluid Phase Equilib.*, 1997, **134**, 285.
 - 48 Y. Qin, X. Yang, Y. Zhu and J. Ping, *J. Phys. Chem. C*, 2008, **112**, 12815–12824.
 - 49 A. Dardin, J. M. DeSimone and E. T. Samulski, *J. Phys. Chem. B*, 1998, **102**, 1775–1780.
 - 50 M. A. Meilchen, B. M. Hasch and M. A. McHugh, *Macromolecules*, 1991, **24**, 4874–4882.
 - 51 T. Huang, J. M. Messman and J. W. Mays, *Macromolecules*, 2008, **41**, 266–268.
 - 52 J. B. McClain, D. Londono, J. R. Combes, T. J. Romack, D. A. Canelas, D. E. Betts, G. D. Wignall, E. T. Samulski and J. M. DeSimone, *J. Am. Chem. Soc.*, 1996, **118**, 917–918.
 - 53 J. M. DeSimone, Z. Guan and C. S. Elsbernd, *Science*, 1992, **257**, 945–947.
 - 54 Y.-L. Hsiao, E. E. Maury, J. M. DeSimone, S. Mawson and K. P. Johnston, *Macromolecules*, 1995, **28**, 8159–8166.
 - 55 P. Lemaire, E. Beckman and R. Enick, *J. Supercrit. Fluids*, 2022, **190**, 105728.
 - 56 J. Xu and R. M. Enick, *OnePetro*, 2001, SPE-84949-PA.
 - 57 R. Enick, E. Beckman, A. Yazdi, V. Krukoni, H. Schonemann and J. Howell, *J. Supercrit. Fluids*, 1998, **13**, 121–126.
 - 58 R. Enick, E. Beckman and A. Hamilton, *Oil & Natural Gas Technology*, 2005, pp. 68–72.
 - 59 A. G. Goicochea and A. Firoozabadi, *J. Phys. Chem. C*, 2019, **123**, 29461–29467.
 - 60 D. Tapriyal, Design of non-fluorous CO₂ soluble compounds, Doctoral dissertation, University of Pittsburgh, 2009, pp. 39–70.
 - 61 C. Dai, P. Liu, M. Gao, Z. Liu, C. Liu, X. Wang, S. Liu, M. Zhao and H. Yan, *J. Mol. Liq.*, 2022, 119563.
 - 62 C. Dai, P. Liu, M. Gao, Z. Liu, C. Liu, Y. Wu, X. Wang, S. Liu, M. Zhao and H. Yan, *J. Mol. Liq.*, 2022, **360**, 119563.
 - 63 W. Sun, B. Sun, Y. Li, X. Huang, H. Fan, X. Zhao, H. Sun and W. Sun, *Polymers*, 2018, **10**, 268.
 - 64 S. Kilic, R. M. Enick and E. J. Beckman, *J. Supercrit. Fluids*, 2019, **146**, 38–46.
 - 65 Z. Huang, C. Shi, J. Xu, S. Kilic, R. M. Enick and E. J. Beckman, *Macromolecules*, 2000, **33**, 5437–5442.



- 66 J. Zhang, L. Q. Rao, S. W. Meng, G. W. Lu, R. Zhang, W. S. Yu and Q. Yang, in *Energy and Sustainability V: Special Contributions*, ed. H. H. AlKaiem, C. A. Brebbia and S. S. Zubir, Wit Press, Southampton, 2015, pp. 175–182.
- 67 D. Rousseau, S. Renard, B. Prempain, C. Féjean and S. Betoulle, in *All Days, SPE*, Tulsa, Oklahoma, USA, 2012, p. SPE-154055-MS.
- 68 J. H. Bae and C. A. Irani, *SPE Adv. Technol. Ser.*, 1993, **1**, 166–171.
- 69 M. Du, X. Sun, C. Dai, H. Li, T. Wang, Z. Xu, M. Zhao, B. Guan and P. Liu, *J. Pet. Sci. Eng.*, 2018, **166**, 369–374.
- 70 M. Zhao, R. Yan, Y. Li, Y. Wu, C. Dai, H. Yan, Z. Liu, Y. Cheng and X. Guo, *Fuel*, 2022, 124358.
- 71 Q. Li, Y. Wang, Q. Li, G. Foster and C. Lei, *RSC Adv.*, 2018, **8**, 8770–8778.
- 72 Q. Li, F. Wang, Y. Wang, B. Bai, J. Zhang, C. Lili, Q. Sun, Y. Wang and K. Forson, *J. Mol. Liq.*, 2023, **376**, 121394.
- 73 Q. Li, Y. Wang, F. Wang, X. Ning, Z. Chuanbao, J. Zhang and C. Zhang, *Environ. Sci. Pollut. Res.*, 2022, **29**, 17682–17694.
- 74 Y. Wang, Q. Li, W. Dong, Q. Li, F. Wang, H. Bai, R. Zhang and A. B. Owusu, *RSC Adv.*, 2018, **8**, 39787–39796.
- 75 M. J. O'Brien, R. J. Perry, M. D. Doherty, J. J. Lee, A. Dhuwe, E. J. Beckman and R. M. Enick, *Energy Fuels*, 2016, **30**, 5990–5998.
- 76 B. Liu, Y. Wang and L. Liang, *Polymers*, 2020, **13**, 78.
- 77 B. Liu, Y. Wang, L. Liang and Y. Zeng, *RSC Adv.*, 2021, **11**, 17197–17205.
- 78 G. Gallo, E. Erdmann and C. N. Cavasotto, *ACS Omega*, 2021, **6**, 24803–24813.
- 79 P. Raveendran and S. L. Wallen, *J. Am. Chem. Soc.*, 2002, **124**, 12590–12599.
- 80 Y. Wang, L. Hong, D. Tapriyal, I. C. Kim, I.-H. Paik, J. M. Crosthwaite, A. D. Hamilton, M. C. Thies, E. J. Beckman, R. M. Enick and J. K. Johnson, *J. Phys. Chem. B*, 2009, **113**, 14971–14980.
- 81 D. Denney, *J. Pet. Technol.*, 2013, **65**, 89–91.
- 82 T. Zhu, H. Gong, M. Dong, Z. Yang, C. Guo and M. Liu, *Fluid Phase Equilib.*, 2018, **458**, 264–271.
- 83 P. N. Khanh and N. T. Trung, in *Carbon Dioxide Chemistry, Capture and Oil Recovery*, ed. I. Karamé, J. Shaya and H. Srou, InTech, 2018.
- 84 J. J. Lee, S. Cummings, A. Dhuwe, R. M. Enick, E. J. Beckman, R. Perry, M. Doherty and M. O'Brien, in *All Days, SPE*, Tulsa, Oklahoma, USA, 2014, p. SPE-169039-MS.
- 85 D. Hu, S. Sun, P.-Q. Yuan, L. Zhao and T. Liu, *J. Phys. Chem. B*, 2015, **119**, 12490–12501.
- 86 D. K. Dandge and J. P. Heller, in *All Days, SPE*, San Antonio, Texas, 1987, p. SPE-16271-MS.
- 87 Y. Zhang, Z. Zhu and J. Tang, *Fluid Phase Equilib.*, 2021, **532**, 112932.
- 88 P. Raveendran and S. L. Wallen, *J. Am. Chem. Soc.*, 2002, **124**, 7274–7275.
- 89 V. K. Potluri, A. D. Hamilton, C. F. Karanikas, S. E. Bane, J. Xu, E. J. Beckman and R. M. Enick, *Fluid Phase Equilib.*, 2003, **211**, 211–217.
- 90 D. Tapriyal, Y. Wang, R. M. Enick, J. K. Johnson, J. Crosthwaite, M. C. Thies, I. H. Paik and A. D. Hamilton, *J. Supercrit. Fluids*, 2008, **46**, 252–257.
- 91 S. E. Conway, H. -S. Byun, M. A. McHugh, J. D. Wang and F. S. Mandel, *J. Appl. Polym. Sci.*, 2001, **80**, 1155–1161.
- 92 J. P. Heller and D. K. Dandge, *US Pat.*, US4607696A, 1986.
- 93 C. Shi, Z. Huang, E. J. Beckman, R. M. Enick, S.-Y. Kim and D. P. Curran, *Ind. Eng. Chem. Res.*, 2001, **40**, 908–913.
- 94 R. M. Enick, *OnePetro*, 1991, SPE-21016-MS.
- 95 P. Gullapalli, J. S. Tsau and J. P. Heller, *OnePetro*, 1995, SPE-28979-MS.
- 96 M. Zhou, H. Tu, Y. He, P. Peng, M. Liao, J. Zhang, X. Xu, W. He, Y. Zhao and X. Guo, *J. Mol. Liq.*, 2020, **312**, 113090.
- 97 M. D. Doherty, J. J. Lee, A. Dhuwe, M. J. O'Brien, R. J. Perry, E. J. Beckman and R. M. Enick, *Energy Fuels*, 2016, **30**, 5601–5610.
- 98 L. Xiaoyu, Plasmonic regulation of photo/photothermal CO₂ catalytic reaction and mechanism, Doctoral dissertation, Shandong University, 2024, pp. 187–194.
- 99 L. Shuo, Fabrication and performance of polyoxyethylene based membrane for CO₂ separation, Doctoral dissertation, Beijing University of Technology, 2023, pp. 85–92.
- 100 D. Tong, Research on regulating electronic structure of copper-sulfur-based electrocatalysts and their performance in carbon dioxide reduction, Doctoral dissertation, Beijing University of Chemical Technology, 2024, pp. 72–79.
- 101 R. D. Shah, in *All Days, SPE*, New Orleans, Louisiana, 2009, p. SPE-129539-STU.
- 102 M. Al-Shargabi, S. Davoodi, D. A. Wood, V. S. Rukavishnikov and K. M. Minaev, *ACS Omega*, 2022, **12**, 9984–9994.
- 103 N. H. Solangi, R. R. Karri, N. M. Mubarak and S. A. Mazari, *Process Saf. Environ. Prot.*, 2024, **185**, 1012–1037.
- 104 O. Olayiwola; N. Coulibaly; N. Liu; B. Guo, *OnePetro*, 2024, SPE-218367-MS.
- 105 A. U. Rognmo, H. Horjen and M. A. Fernø, *Int. J. Greenhouse Gas Control*, 2017, **64**, 113–118.
- 106 G. Gallo and E. Erdmann, in *Day 1 Wed, May 17, 2017, SPE*, Buenos Aires, Argentina, 2017, p. D011S001R003.
- 107 V. Barkhordari and A. Jafari, *J. Water Environ. Nanotechnol.*, 2018, **3**, 12–21.
- 108 S. Davoodi, M. Al-Shargabi, D. A. Wood, V. S. Rukavishnikov and K. M. Minaev, *Fuel*, 2022, **324**, 124669.
- 109 J. L. Dickson, P. S. Shah, B. P. Binks and K. P. Johnston, *Langmuir*, 2004, **20**, 9380–9387.
- 110 P. M. Visintin, R. G. Carbonell, C. K. Schauer and J. M. DeSimone, *Langmuir*, 2005, **21**, 4816–4823.
- 111 P. W. Bell, M. Anand, X. Fan, R. M. Enick and C. B. Roberts, *Langmuir*, 2005, **21**, 11608–11613.
- 112 M. Z. Yates, P. S. Shah, K. P. Johnston, K. T. Lim and S. Webber, *J. Colloid Interface Sci.*, 2000, **227**, 176–184.
- 113 Y. Xu, L. Chen, Y. Zhao, L. M. Cathles and C. K. Ober, *Environ. Sci.:Nano*, 2015, **2**, 288–296.
- 114 J. Zhang, S. Meng*, H. Liu, X. Lv, R. Zhang and B. Yu, in *All Days, SPE*, Nusa Dua, Bali, Indonesia, 2015, p. SPE-176221-MS.



Review

- 115 R. Khaledialidusti, A. K. Mishra and A. Barnoush, *J. Chem. Phys.*, 2018, **149**, 224702.
- 116 Z. Su, L. Yang, N. Zhao, J. Song, X. Li and X. Wu, *Appl. Therm. Eng.*, 2024, **241**, 122347.
- 117 Y. Wang, B. Liu, D. Li and L. Liang, *Energy Sources, Part A*, 2022, **44**, 6602–6617.
- 118 A. Gandomkar and M. Sharif, *J. Pet. Sci. Eng.*, 2020, **194**, 107491.
- 119 L. Thomas, H. Tang, D. M. Kalyon, S. Aktas, J. D. Arthur, J. Blotevogel, J. W. Carey, A. Filshill, P. Fu, G. Hsuan, T. Hu, D. Soeder, S. Shah, R. D. Vidic and M. H. Young, *J. Pet. Sci. Eng.*, 2019, **173**, 793–803.
- 120 Y. Feng, K. Haugen and A. Firoozabadi, *J. Geophys. Res.:Solid Earth*, 2021, **126**, e2021JB022509.
- 121 M. Sedghi and L. Goual, *OnePetro*, 2016, SPE-179040-MS.

